molecules

MDPI

Article

Baicalin Alleviates Rheumatoid Arthritis by Suppressing Crosstalk Between RA-FLSs and Synovial Macrophages via the CCL2–CCR2–MAPK/NF-κB Signaling Network

Jing Wang [1,2,†], Maiyan Hai [1,2,†], Haiyan He [1,2,†], Wenxuan Zhang [1,2], Yuxin Yang [1], Wei Zhang [1], Wenwei Gao [1], Miao Sun [1], Rui Ma [1,2,*] and Qiaofeng Wan [1,2,*]

[1] Department of Pathogenic Biology and Immunology, College of Basic Medical Science, Ningxia Medical University, Yinchuan 750004, China; 17835684863@163.com (J.W.); hmyhmy0821@126.com (M.H.); 17795077219@163.com (H.H.); 15589966339@163.com (W.Z.); yangyuxin19971002@126.com (Y.Y.); zhangwei@nxmu.edu.cn (W.Z.); 19890033@nxmu.edu.cn (W.G.); nxsunm@126.com (M.S.)
[2] Ningxia Key Laboratory of Infection and Immunity, Yinchuan 750004, China
* Correspondence: mr_312@126.com (R.M.); wanqiaofeng@nxmu.edu.cn (Q.W.)
† These authors contributed equally to this work.

Abstract

Rheumatoid arthritis (RA) is a chronic autoimmune inflammatory disorder driven by abnormal interactions between fibroblast-like synoviocytes (RA-FLSs) and synovial macrophages, leading to sustained synovitis. Although transcriptomic evidence reveals that baicalin mainly regulates the mitogen-activated protein kinase (MAPK) and NF-κB pathways, its role in mediating crosstalk between RA-FLSs and synovial macrophages remains poorly defined. This study aimed to elucidate whether the therapeutic effect of baicalin against collagen-induced arthritis (CIA) is associated with disruption of the crosstalk between RA-FLSs and synovial macrophages via the CCL2–CCR2–MAPK/NF-κB signaling network. In vivo treatment confirmed that baicalin inhibited the signaling cascade and promoted macrophage M2 polarization. CCR2-knockdown ($CCR2^{KD}$) and -overexpressing ($CCR2^{OE}$) macrophage cell lines were constructed using lentivirus. Experiments with $CCR2^{KD}$/$CCR2^{OE}$ macrophages and an RA-FLS co-culture system showed that baicalin downregulated CCL2's release from RA-FLSs, blocking macrophage migration. Both M1 macrophages and RA-FLSs pretreated with baicalin were capable of suppressing proinflammatory cytokine secretion from their respective interacting partners through this signaling axis, showing that baicalin suppressed excessive inflammatory cytokine secretion by disrupting RA-FLS-synovial macrophage crosstalk via a CCL2–CCR2–MAPK/NF-κB signaling network, which may represent the principal mechanism underlying the baicalin-mediated amelioration of RA. These findings offer new insights into baicalin's anti-arthritic mechanism.

Keywords: baicalin; rheumatoid arthritis; synovial fibroblasts; synovial macrophages; crosstalk

Check for updates

Academic Editor: C. Michael Greenlief

Received: 19 October 2026
Revised: 9 November 2026
Accepted: 12 November 2026
Published: 15 November 2026

Copyright: © 2026 by the authors. Licensee MDPI, Basel, Switzerland. This article is an open access article distributed under the terms and conditions of the Creative Commons Attribution (CC BY) license.

1. Introduction

Rheumatoid arthritis (RA) is a persistent autoimmune disorder marked by systemic inflammation, characterized by progressive synovial hyperplasia and irreversible joint structural damage leading to joint deformity and functional disability [1]. The global disease burden of RA keeps rising, and it affects approximately 0.3 to 1.2% of the world's population and markedly shortens patients' lifespans by more than a decade [2,3]. Predictions based on the Global Burden of Disease projections forecast that RA will remain a major public health

threat, affecting an estimated 317,000 people globally by 2050 [4]. These data underscore an urgent need for effective RA therapeutic regimens.

Although the exact pathogenesis of RA remains incompletely elucidated, accumulating evidence demonstrates that genetic factors, environmental stimuli, and immune dysregulation collectively drive RA progression [5,6]. RA-fibroblast-like synoviocytes (RA-FLSs) and synovial macrophages are pivotal effector cells responsible for RA pathogenesis [7,8]. The excessive activation of these two cell types and the subsequent uncontrolled release of intra-articular proinflammatory cytokines act as core pathological drivers of RA progression [9,10]. In the RA microenvironment, dysregulated cytokine secretion breaks immune tolerance, induces immune dysfunction, and ultimately triggers persistent autoimmune inflammation [11,12]. Furthermore, the cytokine-abundant synovial microenvironment facilitates bidirectional crosstalk between RA-FLSs and synovial macrophages [13,14]. M1-polarized synovial macrophages release abundant proinflammatory cytokines, triggering the abnormal activation of RA-FLSs [15]. In return, activated RA-FLSs further promote M1 macrophage polarization, forming a positive feedback loop that continuously amplifies synovial inflammation [16,17]. Such synergistic proinflammatory interactions between the two cell types dominate the persistent deterioration observed in RA [18].

The CCL2–CCR2 signaling cascade acts as a crucial regulatory pathway that modulates macrophage recruitment and activation during RA pathogenesis [19]. CCR2 is a pivotal surface receptor governing macrophage proliferation, migration, and inflammatory activation [20,21]. CCL2, the primary endogenous ligand of CCR2, is highly secreted by injured RA-FLSs in the early stage of synovitis [22]. The binding interaction between CCL2 and CCR2 recruits circulating macrophages to inflamed synovial tissues, further triggering the activation of downstream inflammatory signaling cascades, including the MAPK and NF-κB pathways [23,24]. The MAPK subfamilies (P38, ERK, and JNK) are central mediators of inflammatory signal transduction, and suppressing the phosphorylation of these proteins efficiently inhibits CCL2 production [25]. As a master inflammatory transcription factor, NF-κB regulates the expression of CCL2, CCR2, and multiple downstream inflammatory mediators, highlighting the critical regulatory role of the CCL2–CCR2–MAPK/NF-κB signaling axis in RA inflammatory progression [26].

Although recent disease-modifying antirheumatic drugs (DMARDs) can relieve inflammatory symptoms and slow disease progression, their widespread clinical use is limited by their high costs and inevitable adverse side effects [27,28]. Hence, it is imperative to develop novel anti-RA candidates with low toxicity and affordable clinical value. Baicalin (7-glucuronic acid,5,6-dihydroxyflavone), the principal bioactive component derived from *Scutellaria baicalensis* Georgi(Lamiaceae), possesses potent anti-inflammatory and immunomodulatory capacities, with favorable biosafety profiles [29–32].

Our previous studies proved that 60 mg/kg/d baicalin relieves joint inflammation via the MAPK/NF-κB pathways in collagen-induced arthritis (CIA) rats [33]. A schematic diagram illustrating the CCL2/CCR2/MAPK/NF-κB signaling network and the putative targets of baicalin is presented in Figure 1. In the present study, CIA rat models were used to explore whether the anti-RA activity of baicalin is associated with the suppression of the CCL2–CCR2–MAPK/NF-κB pathways and promotion of macrophage polarization from the M1 to M2 phenotype, and cellular experiments were then conducted to explore whether baicalin suppresses excessive inflammatory cytokine secretion by blocking crosstalk between RA-FLSs and synovial macrophages via the CCL2–CCR2–MAPK/NF-κB signaling network.

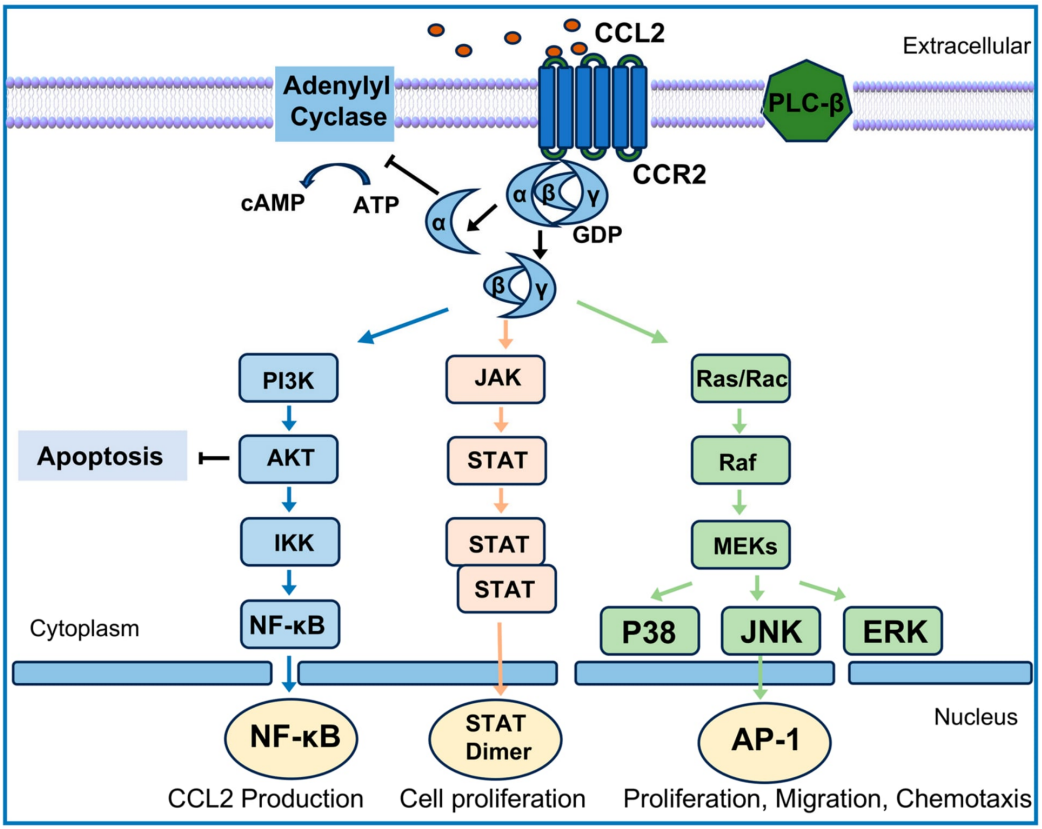


Figure 1. Schematic diagram illustrating the CCL2–CCR2–MAPK/NF-κB signaling network and the potential molecular targets of baicalin.

2. Materials and Methods

2.1. Induction of Collagen-Induced Arthritis (CIA) and Animal Treatment

Twenty-four male Sprague–Dawley (SD) rats (6–7 weeks, 200 ± 10 g) were obtained from the Laboratory Animal Center of Ningxia Medical University (SCXK 2020-0001). All animal procedures were conducted in a specific pathogen-free facility (22 ± 2 °C, 55 ± 5% humidity, 12 h light–dark cycle) and approved by the Animal Ethics Committee of Ningxia Medical University (2023-N0023, 8 March 2023), following institutional animal welfare guidelines. After one week of acclimatization, rats were randomized into four groups ($n = 6$ per group): a blank control group, CIA model group, baicalin group (#25091005, Kehua AI, Shenzhen, China), and dexamethasone (DEX) positive control group (#H41020035, Sinopharm Rongsheng, Jiaozuo, China). CIA was induced by the subcutaneous injection of 0.1 mL of bovine type II collagen (#20022, Chondrex, Inc., Woodinville, WA, USA) emulsified with complete Freund's adjuvant (#7001, Chondrex, Inc., Woodinville, USA) at the tail base and hind footpads; booster immunization was administered on day 7. From day 21 post-modeling, the rats received daily intraperitoneal administration: baicalin (60 mg/kg), DEX (0.5 mg/kg), or equivalent normal saline (2 mL/day) for normal/model groups. Body weight and paw swelling were monitored weekly (day 0–21) and then every three days until day 42. Animals were sacrificed on day 43 (Figure 2A). The serum was separated from collected blood. Knee synovial tissues, ankle joints, and spleens were harvested, and the spleen wet weights were recorded. Tissues were snap-frozen in liquid nitrogen and stored at −80 °C for downstream biochemical and molecular tests.

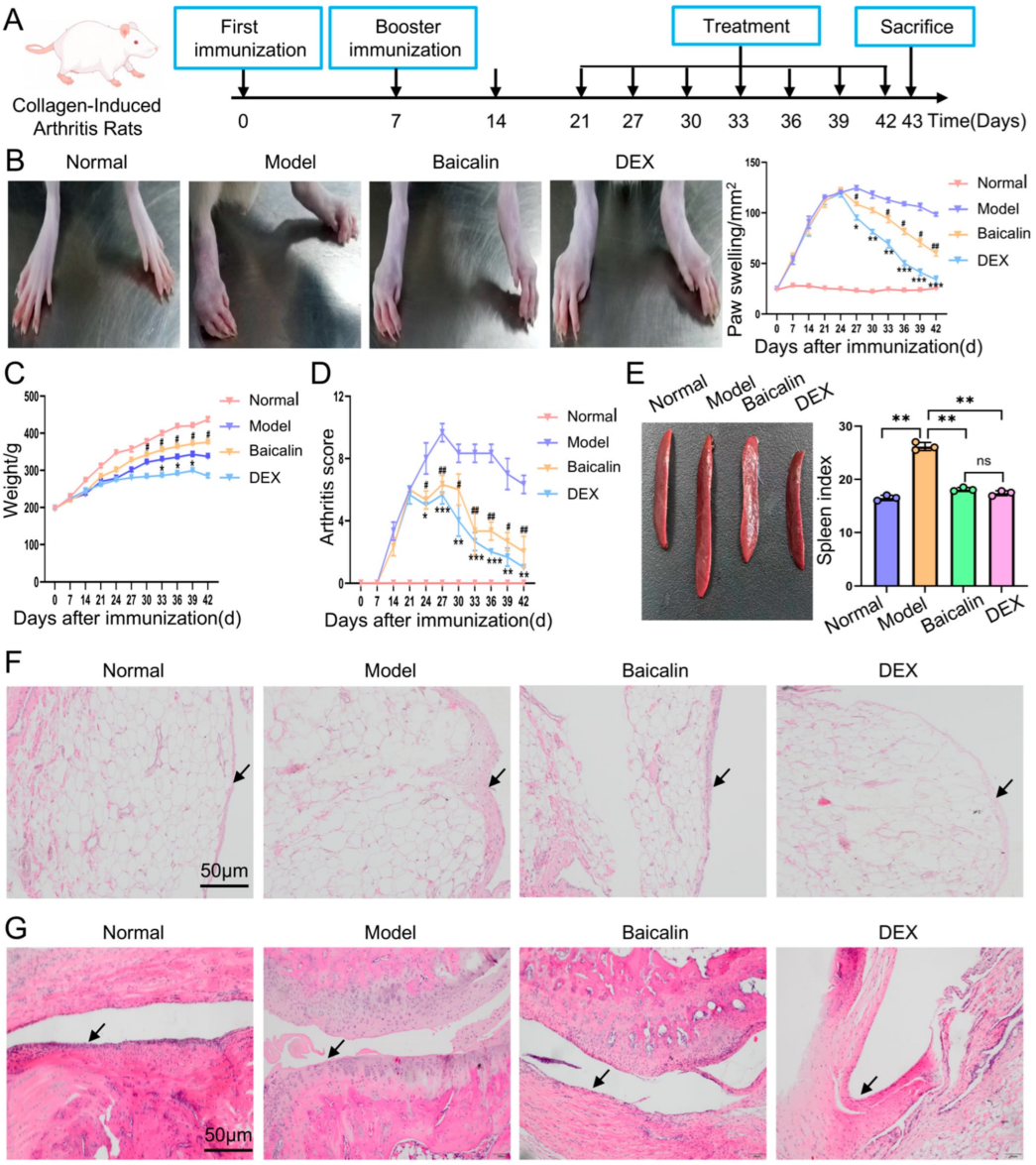


Figure 2. Baicalin alleviates arthritis severity in collagen-induced arthritis (CIA) rats. Twenty-four CIA model rats were divided into 4 groups (n = 6 per group): Normal control group (Normal), CIA model group (Model), Baicalin treatment group (Baicalin), Dexamethasone treatment group (DEX). (**A**) Schematic diagram of experimental treatments. Starting on day 21 after modeling, rats received daily intraperitoneal injection of corresponding treatments: 60 mg/kg baicalin for the Baicalin group, 0.5 mg/kg DEX for the DEX group, and equal volumes of normal saline for the Normal and Model groups. (**B**) Quantitative analysis of paw swelling. (**C**) Changes in body weight. (**D**) Evaluation of arthritis scores. (**E**) Detection of spleen index. (**F**,**G**) Hematoxylin and eosin (H&E) staining of knee and ankle synovial tissues, respectively; arrows indicate the synovial layer. * $p < 0.05$, ** $p < 0.01$, *** $p < 0.001$ vs. the Model group; # $p < 0.05$, ## $p < 0.01$, $p < 0.001$ vs. model group; ns, not significant.

2.2. Anesthesia and Euthanasia Procedures for CIA Rats

Prior to all invasive procedures, CIA rats were deeply anesthetized via the intraperitoneal injection of sodium pentobarbital (45 mg/kg body weight). Adequate anesthetic depth was confirmed by loss of the corneal reflex, full muscle relaxation, the absence of spontaneous movement, and regular stable respiration. The rats were kept on a thermostatically controlled heating pad to maintain their core body temperature, with continuous monitoring of vital signs until sampling was finished. At the predefined experimental endpoint, all rats were humanely euthanized using the same pentobarbital anesthesia

regimen. Following intracardiac blood collection, irreversible death was verified by the permanent cessation of vital signs, and tissues including the spleen and synovial membrane were harvested for subsequent assays. All animal procedures were performed by trained qualified personnel and complied with the AVMA Guidelines for the Humane Euthanasia of Laboratory Animals to minimize animal pain and distress.

2.3. Spleen Index Measurement

The spleen index was adopted as a key biomarker reflecting immune status to evaluate the immunomodulatory potential, which was calculated according to the standard formula: Spleen index (mg/g) = spleen wet weight (mg)/body weight (g).

2.4. Histological Analysis

Briefly, synovial tissues harvested from rat knee and ankle joints were fixed in 4% paraformaldehyde for 24 h. Ankle joints were then decalcified in an EDTA (ethylenediamine tetraacetic acid)–formalin decalcifying solution (#BL518A, Biosharp, Hefei, China) for 2 months, with the solution refreshed once weekly. Following paraffin embedding, synovial and joint tissues were sectioned at 5 μm thickness and subjected to hematoxylin and eosin (H&E) staining. Histological observation and pathological evaluation were performed under a light microscope.

2.5. Flow Cytometric Analysis of Macrophages Polarized In Vitro and In Vivo

Spleen tissues were rapidly homogenized under low-temperature and sterile conditions. Lymphocytes were subsequently isolated to prepare single-cell suspensions, and were then stained with fluorescence-labeled specific antibodies targeting CD11b (#BE-05168401, Bioss, Beijing, China), F4/80 (#sc-377009, SCBT, Dallas, TX, USA), CD86 (#743211, Thermo Fisher, Waltham, MA, USA), and CD206 (#sc-58986, SCBT, Dallas, USA).

J774A.1 cells were seeded into six-well plates at a density of 5×10^5 cells per well and cultured for 24 h. Subsequently, cells were stimulated with 10 pg/mL lipopolysaccharide (LPS) (#S1732, Beyotime, Shanghai, China) combined with 20 ng/mL IFN-γ (#KGD1284-100, Beyotime, China) for another 48 h, and were then stained with fluorescence-labeled specific antibodies targeting CD11b (#17-0112-82, Thermo Fisher, USA), F4/80 (#45-4801-82, Thermo Fisher, USA), CD86 (#12-0862-82, Thermo Fisher, USA), and CD206 (#365-2061-82, Thermo Fisher, USA).

The proportions of M1 and M2 macrophages among stained lymphocytes and J774A.1 cells treated with LPS and IFN-γ were analyzed using a CytoFLEX flow cytometer (Attune NxT, Thermo Fisher, USA). $F4/80^+CD11b^+$cells were defined as macrophages where the $CD86^+CD206^-$population represented M1 macrophages, while the $CD86^-CD206^+$population represented M2 macrophages.

2.6. Cells and Cell Treatment

2.6.1. Cell Source

Human rheumatoid arthritis fibroblast-like synoviocytes (RA-FLSs, #GD-C0038632A65-921) were purchased from SGD Bio (Shanghai, China), Ltd. The cell identity and purity were verified by the manufacturer, as documented in the certificate of analysis. The murine monocyte–macrophage J774A.1 cell line (#GD-C00135787) was also obtained from SGD Bio (Shanghai, China).

Both RA-FLSs and J774A.1 cells were cultured in high-glucose DMEM supplemented with 10% fetal bovine serum and 1% penicillin–streptomycin, at 37 °C in a humidified incubator with 5% CO_2. Cells at passages 3–5 were used for in vitro experiments, and mycoplasma contamination was routinely excluded.

2.6.2. Construction of CCR2-Knockdown ($CCR2^{KD}$) and CCR2-Overexpressing ($CCR2^{OE}$) Stable J774A.1 Macrophage Cell Lines

Lentiviruses for $CCR2^{KD}$ and $CCR2^{OE}$ were synthesized by GeneChem (Shanghai, China). First, J774A.1 cells were assigned to three groups: Control group (complete medium); Enhancer A group (complete medium + enhancer A); Enhancer P group (complete medium + enhancer P). After approximately 72 h of infection, the cells were observed under a fluorescence microscope. Conditions yielding abundant fluorescence, 80% infection efficiency, and favorable cell viability were adopted for subsequent transduction experiments.

J774A.1 cells were transduced with the viral supernatants of the negative control (NC), three CCR2-knockdown constructs ($CCR2^{KD1}$, $CCR2^{KD2}$, $CCR2^{KD3}$), and a CCR2-overexpression construct ($CCR2^{OE}$) for 24 h. The cellular fluorescence intensity was then examined. Stable cell pools were selected with puromycin-containing medium for 2–3 weeks, followed by culture in complete medium before protein extraction for validation. To validate $CCR2^{KD}$ stable lines, five groups were established: control (wild-type J774A.1), NC, $CCR2^{KD1}$, $CCR2^{KD2}$, and $CCR2^{KD3}$. CCR2 expression was quantified via Western blotting, and the clone with optimal knockdown efficiency was selected for further experiments. To validate the $CCR2^{OE}$ stable line, three groups including control, NC, and $CCR2^{OE}$ were used, and $CCR2^{OE}$ was confirmed by Western blotting.

2.6.3. Effects of Baicalin-Pretreated RA-FLSs on Macrophage Migration Through the CCL2–CCR2 Axis

First, RA-FLSs were preincubated with 50 μg/mL baicalin in culture flasks for 72 h. Subsequently, untreated RA-FLSs and baicalin-pretreated RA-FLSs were seeded into 24-well plates at 5×10^4 cells/well, followed by co-culture with wild-type J774A.1 cells, negative control lentivirus-transfected J774A.1 cells, and $CCR2^{KD}$ and $CCR2^{OE}$ J774A.1 cells, which were seeded into Transwell inserts at 5×10^4 cells/well. The experiment included eight groups (three replicates each) with two harvesting time points at 24 h and 48 h. The group assignments were as follows: ① Control: wild-type J774A.1 + untreated RA-FLSs; ② Baicalin: wild-type J774A.1 + baicalin-pretreated RA-FLSs; ③ NC: negative control lentivirus-transfected J774A.1 + untreated RA-FLSs; ④ NC + Baicalin: negative control lentivirus-transfected J774A.1 + baicalin-pretreated RA-FLSs; ⑤ $CCR2^{KD}$: $CCR2^{KD}$J774A.1 + untreated RA-FLSs; ⑥ $CCR2^{KD}$ + Baicalin: $CCR2^{KD}$ J774A.1 + baicalin-pretreated RA-FLSs; ⑦ $CCR2^{OE}$: $CCR2^{OE}$J774A.1 + untreated RA-FLSs; ⑧ $CCR2^{OE}$ + Baicalin: $CCR2^{OE}$ J774A.1 + baicalin-pretreated RA-FLSs. After 24 h and 48 h of co-culture, the Transwell inserts were removed and washed three times with PBS. The inserts were fixed in 4% paraformaldehyde at room temperature for 30 min, followed by three additional PBS washes. Then, 500 μL of 0.5% crystal violet staining solution was added to each insert for 15 min of staining. Excess crystal violet was rinsed off with PBS, and cells that had not migrated through the membrane were gently wiped away from the upper chamber using cotton swabs. Five non-overlapping fields of view were randomly selected per insert for imaging under a light microscope, and the number of migrated cells was quantified using ImageJ (version 1.54g) software. Culture supernatants from each group were collected, and CCL2 expression was measured by ELISA.

2.6.4. Effects of Baicalin-Pretreated M1 Macrophages on Secretion of Inflammation-Related Factors from RA-FLSs via the CCL2–CCR2–MAPK/NF-κB Signaling Axis

Firstly, J774A.1 macrophages were stimulated with 10 pg/mL LPS and 20 ng/mL IFN-γ for 48 h to induce M1-type polarization. Subsequently, the M1-polarized J774A.1 macrophages were treated with baicalin at concentrations of 25 μg/mL and 50 μg/mL

for 72 h. Thereafter, untreated M1-polarized J774A.1 macrophages, 25 μg/mL baicalin-pretreated M1-polarized J774A.1 macrophages, and 50 μg/mL baicalin-pretreated M1-polarized J774A.1 macrophages were seeded into Transwell inserts at a density of 2×10^5 cells/well. Meanwhile, untreated RA-FLSs were inoculated in 6-well plates at the same cell density. The experiment included 3 groups (three replicates each) with one harvesting time point at 48 h. The group assignments were as follows: ① 0 μg/mL baicalin: M1-polarized J774A.1 + RA-FLSs; ②25 μg/mL baicalin: 25 μg/mL baicalin-pretreated M1-polarized J774A.1 + RA-FLSs; ③ 50 μg/mL baicalin: 50 μg/mL baicalin-pretreated M1-polarized J774A.1 + RA-FLSs. After 48 h of co-culture, culture supernatants from each group were collected, and the IL-6, IL-10, and CCL2 concentrations were measured by ELISA; total protein was extracted from RA-FLSs in each group, and the expression levels of CCR2 (#AF2359, Beyotime, China), NF-κB (#AN365-1, Beyotime, China), p-P38/P38 (#ER2001-52, #ET1702-65, HUABIO, Hangzhou, China), p-JNK/JNK (#ET1609-42, #ET1601-28, HUABIO, China) and p-ERK/ERK (#sc-7383, #ET1601-29, HUABIO, China) were analyzed by Western blotting.

2.6.5. Effects of Baicalin-Pretreated RA-FLSs on Secretion of Inflammation-Related Factors from M1 Macrophages via the CCL2–CCR2–MAPK/NF-κB Signaling Axis

RA-FLSs were incubated with baicalin at 25 μg/mL and 50 μg/mL for 72 h. Subsequently, baicalin-untreated RA-FLSs (0 μg/mL baicalin), 25 μg/mL baicalin-pretreated RA-FLSs, and 50 μg/mL baicalin-pretreated RA-FLSs were seeded into Transwell inserts at a density of 2×10^5 cells/well. Untreated M1-polarized J774A.1 macrophages were seeded in 6-well plates at the same cell density. Three experimental groups were set up, with three biological replicates per group, and samples were harvested at the 48 h time point. The group settings were as follows: ① 0 μg/mL baicalin: RA-FLSs + M1-polarized J774A.1; ② 25 μg/mL baicalin: 25 μg/mL baicalin-pretreated RA-FLSs + M1-polarized J774A.1; ③ 50 μg/mL baicalin: 50 μg/mL baicalin-pretreated RA-FLSs + M1-polarized J774A.1. Following 48 h of co-culture, cell culture supernatants from each group were collected, and the levels of IL-6, IL-10, and CCL2 were quantified using ELISA. Total protein was extracted from M1-polarized J774A.1 macrophages in each group, and the protein expression of CCR2, NF-κB, p-P38/P38, p-JNK/JNK, and p-ERK/ERK was determined via Western blotting.

2.7. Enzyme-Linked Immunosorbent Assay (ELISA)

Commercial ELISA kits were applied to quantify the concentrations of CCL2, IL-1β, IL-6, IL-17A, and IL-10 (#JL20882, #JL20884, #JL20896, #JL20880, #JL13427, Shanghai Jianglai Biotechnology, Shanghai, China) in the serum, as well as IL-6, IL-10, and CCL2 (#JM-11575M1, #JM-11576M1, #JM-11572M1, Jingmei (Yancheng, China) levels in cell culture supernatants. All experimental procedures were carried out in strict compliance with the manufacturer's standard protocols.

2.8. Western Blotting Analysis

Total proteins were extracted from rat synovial tissues and cultured cells using cell lysis buffer containing protease inhibitors. The protein concentration of each sample was quantified via a BCA protein assay kit according to standard protocols. Extracted protein samples were then separated electrophoretically using 10% SDS–polyacrylamide gels, followed by electrotransfer onto polyvinylidene fluoride (PVDF) membranes. The transferred membranes were blocked with rapid blocking solution to eliminate non-specific binding. Subsequently, the membranes were incubated with primary antibodies at 4 °C overnight. After thorough rinsing with TBST buffer, the membranes were probed with matched secondary

antibodies at 37 °C for 60 min. Finally, immunoreactive protein bands were visualized using ECL chemiluminescence reagents to detect target protein expression levels.

2.9. Statistical Analysis

All experimental results were presented as mean ± standard deviation. Statistical analysis was carried out with GraphPad Prism 6 software (GraphPad Software, Inc., San Diego, CA, USA). One-way analysis of variance (ANOVA) was adopted for comparison across three experimental groups, and Dunnett's multiple comparison test was applied for pairwise comparisons between two groups. A difference with $p < 0.05$ was considered statistically significant.

3. Results

3.1. Baicalin Attenuates Inflammatory Injury in CIA Rats

To evaluate the therapeutic effect of baicalin on rheumatoid arthritis, the rat hind paw swelling degree, body weight, and clinical arthritis scores were dynamically monitored throughout the entire experimental course. Compared with model rats, rats treated with baicalin exhibited a marked reduction in paw swelling starting at day 27 (Figure 2B). Persistent inflammatory insult retarded body weight gain in CIA rats, while baicalin treatment markedly reversed model-related weight loss starting at day 30 (Figure 2C). Consistent with the alleviated paw swelling, treatment with baicalin markedly lowered clinical arthritis scores in CIA rats starting at day 24 compared with the model group (Figure 2D). The spleen index was significantly decreased in the baicalin-treated group compared to the model group (Figure 2E). H&E staining of synovial tissues isolated from the knee and ankle joints of CIA rats revealed that the normal group exhibited a normal synovium appearance, whereas the model group demonstrated notable histological abnormalities, including synovial thickening, inflammatory cell infiltration, and excessive proliferation of synovial fibroblasts. Compared with the model group, baicalin-treated rats displayed improvements in histological changes, further indicating the beneficial effect of baicalin on collagen-induced joint injury (Figure 2F,G). In addition, baicalin led to no significant differences compared with the DEX group in terms of paw swelling, the arthritis index, the spleen index, and synovial inflammatory infiltration. In summary, baicalin has reliable anti-arthritic activity, which can effectively relieve joint swelling and alleviate synovial inflammatory damage in CIA rats.

3.2. The Anti-Arthritic Effect of Baicalin Is Associated with Blockade of the CCL2–CCR2–MAPK/NF-κB Signaling Cascade and Induction of M2-Type Macrophage Polarization

We sought to investigate whether the anti-arthritic efficacy of baicalin against RA was linked to the suppression of CCL2–CCR2–MAPK/NF-κB signaling pathway activation and the induction of macrophage polarization toward the M2 phenotype. The expression profiles of core proteins associated with the CCL2–CCR2 axis, MAPK signaling cascade, and NF-κB inflammatory pathway were quantified using Western blotting analysis. In contrast to the normal group, model rats exhibited distinct upregulation of CCR2 protein expression; elevated phosphorylation of P38, ERK, and JNK; and increased NF-κB protein abundance, suggesting the robust activation of inflammatory signaling in CIA rats. Both baicalin and dexamethasone interventions could efficiently block the overactivation of these signaling pathways. Specifically, the abnormally high expression of CCR2, phosphorylated MAPK family members (p-P38/P38, p-ERK/ERK, p-JNK/JNK), and NF-κB was effectively suppressed after baicalin or DEX intervention. Meanwhile, no substantial difference was found in protein levels between the baicalin and DEX treatment groups

(Figure 3A). ELISA-based serum biochemical measurements revealed substantially higher serum concentrations of CCL2, IL-1β, IL-6, and IL-17A in CIA model rats, whereas IL-10 was markedly downregulated compared with normal rats. Relative to model rats, baicalin lowered circulating proinflammatory CCL2, IL-1β, IL-6, and IL-17A, and prominently elevated IL-10. No significant differences in any serum parameter were detected between the baicalin group and DEX group (Figure 3B). Analytical data from flow cytometry demonstrated that, compared with the model group, rats administered baicalin presented a lower proportion of proinflammatory M1 macrophages and a prominently higher proportion of anti-inflammatory M2 macrophages (Figure 3C). This study indicates that anti-arthritic efficacy of baicalin against RA is closely related to its capacity to inhibit the overactivation of the CCL2–CCR2–MAPK/NF-κB signaling cascade and facilitate macrophage polarization toward the anti-inflammatory M2 phenotype.

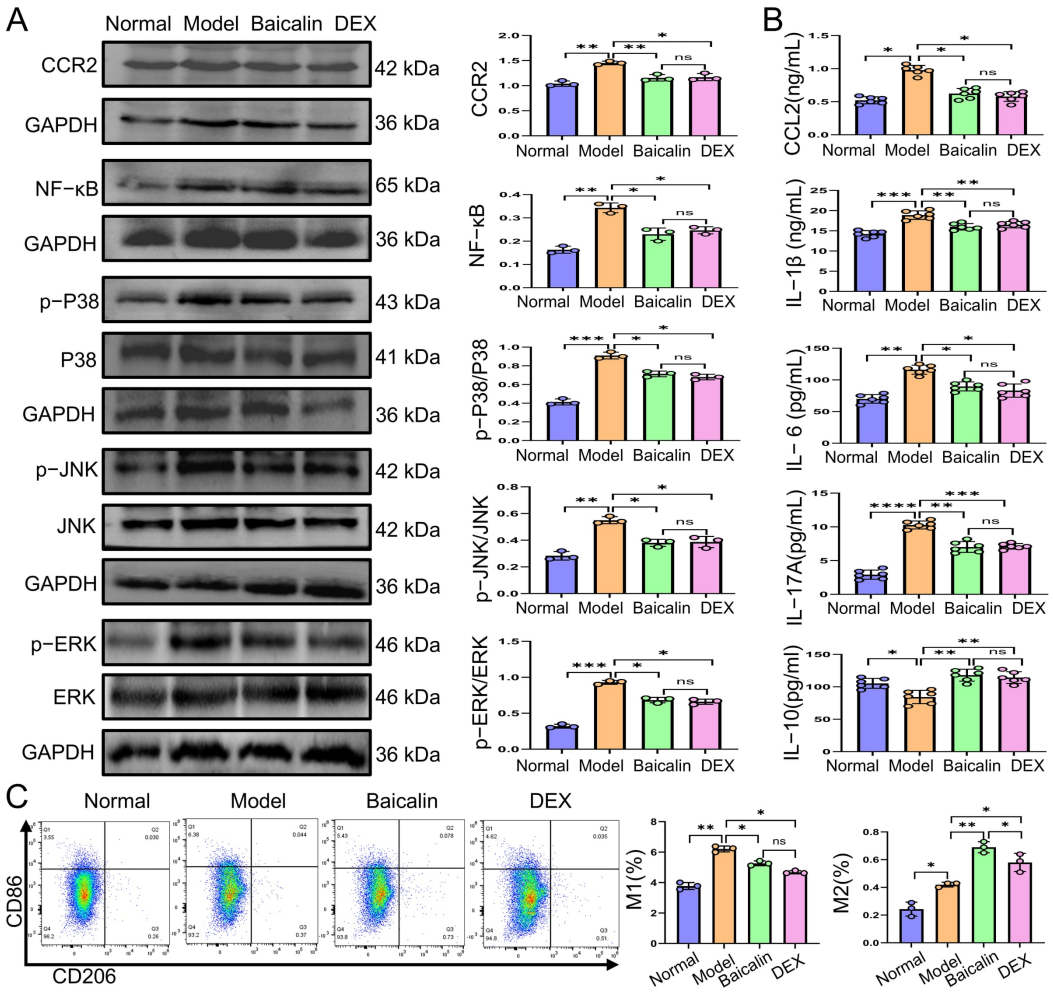


Figure 3. The therapeutic effects of baicalin against RA are closely associated with suppression of CCL2–CCR2–MAPK/NF-κB signaling activation and induction of macrophage polarization toward the M2 phenotype. (**A**) Protein expression levels of key components in the CCL2–CCR2–MAPK/NF-κB axis in synovial tissues: CCR2, NF-κB, p-P38/P38, p-ERK/ERK, and p-JNK/JNK. (**B**) Serum concentrations of CCL2, IL-1β, IL-6, IL-17A and IL-10. (**C**) Macrophage polarization. F4/80^{+}CD11b^{+} cells were identified as macrophages: CD86^{+}CD206^{-} for M1-type and CD86^{-}CD206^{+}for M2-type macrophages. * $p < 0.05$, ** $p < 0.01$, *** $p < 0.001$, **** $p < 0.0001$; ns, not significant.

3.3. J774A.1 Macrophage Cell Lines with Stable CCR2^{KD} or CCR2^{OE} Were Successfully Constructed

Fluorescence microscopy imaging was utilized to screen the optimal experimental parameters for lentivirus infection in J774A.1 macrophages. When the infection multiplicity was MOI = 50 and the infection enhancer was P, the infection efficiency reached 80%. This condition was selected as the optimal infection condition for lentivirus (Figure 4A). Following lentivirus transfection, Western blot assays were carried out to validate the efficiency of CCR2^{KD3} in constructed cell models. Compared with the negative control NC group, the CCR2^{KD1} fragment failed to produce an obvious inhibitory effect on CCR2 protein expression. In contrast, the CCR2^{KD2} and CCR2^{KD3} sequences significantly reduced endogenous CCR2 levels, respectively. Among these two effective interfering sequences, CCR2^{KD2} yielded a more potent knockdown effect, and was therefore chosen for subsequent cellular functional experiments (Figure 4B). For the overexpression model, the *CCR2^{OE}* group displayed distinctly elevated CCR2 expression compared with the NC group (Figure 4C). The above results confirm the successful generation of stable CCR2^{KD} and CCR2^{OE} macrophage cell lines.

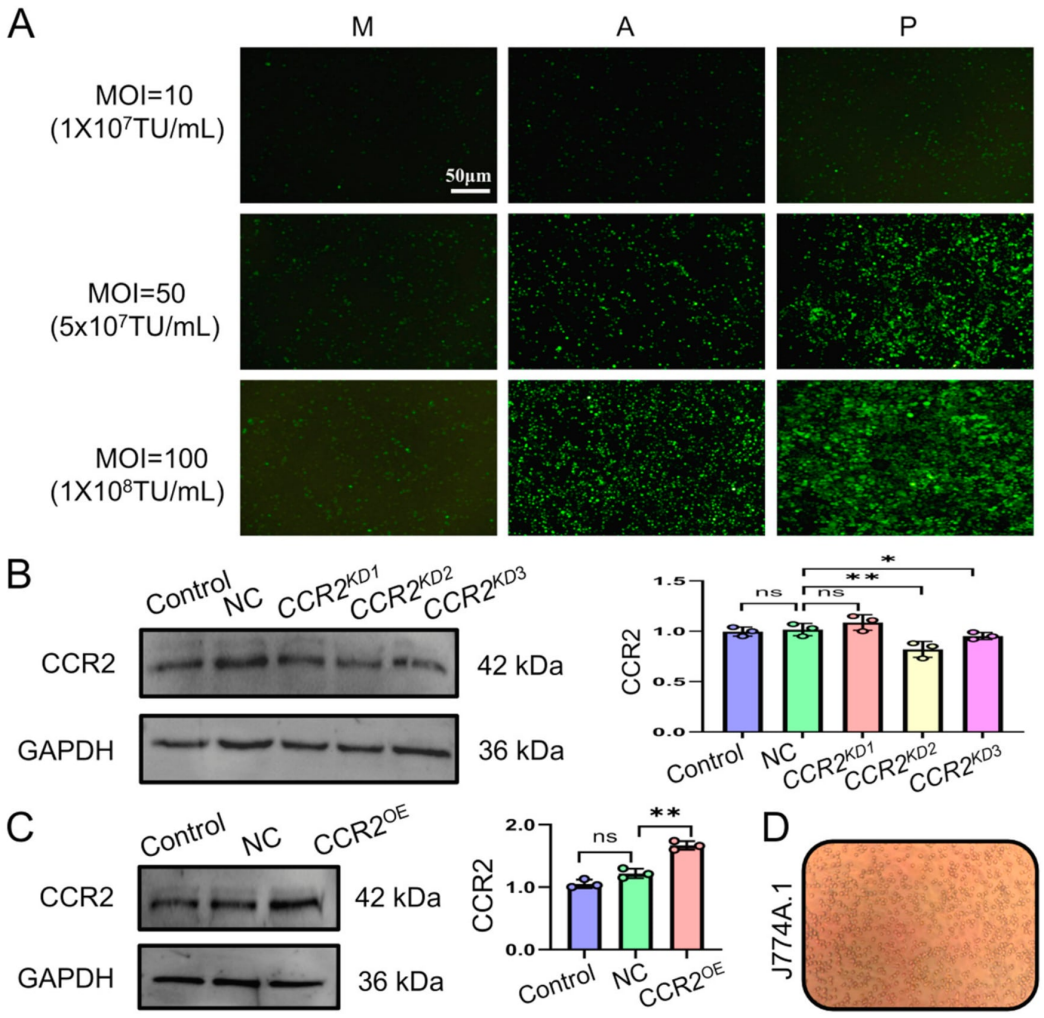


Figure 4. Construction of CCR2^{KD} and CCR2^{OE} stable J774A.1 macrophage cell lines. (**A**) Fluorescence microscopy images of lentiviral infection efficiency. M: Control group; A: Enhancer A group; P: Enhancer P group. (**B**) Western blotting analysis of stable CCR2^{KD} macrophage cell line. Control: Blank control group; NC: Negative control group; CCR2^{KD1}: CCR2 knockdown group 1; CCR2^{KD2}: *CCR2* knockdown group 2; CCR2^{KD3}: *CCR2* knockdown group 3. (**C**) Western blotting analysis of stable CCR2^{OE} macrophage cell lines. Control: Blank control group; NC: Negative control group;

$CCR2^{OE}$: *CCR2* overexpression group. (**D**) Cultured J774A.1 macrophages. * $p < 0.05$, ** $p < 0.01$ vs. NC group; ns, not significant.

3.4. Baicalin-Pretreated RA-FLSs Suppress Macrophage Migration via CCL2–CCR2 Axis

A J774A.1 macrophage migration experiment demonstrated that the migratory abilities of $CCR2^{KD}$ and $CCR2^{OE}$ macrophages were obviously suppressed following 24 h co-culture with baicalin-pretreated RA-FLSs (Figure 5A,B). The ELISA results for CCL2 levels in the 24 h co-culture system showed that CCL2 levels were significantly downregulated in all the baicalin-treated groups compared with their control group (Figure 5C). The 48 h co-culture yielded results consistent with those obtained at 24 h (Figure 5D–F). This study demonstrates that baicalin inhibits CCL2 secretion from RA-FLSs, thereby restraining macrophage migration via the CCL2–CCR2 axis.

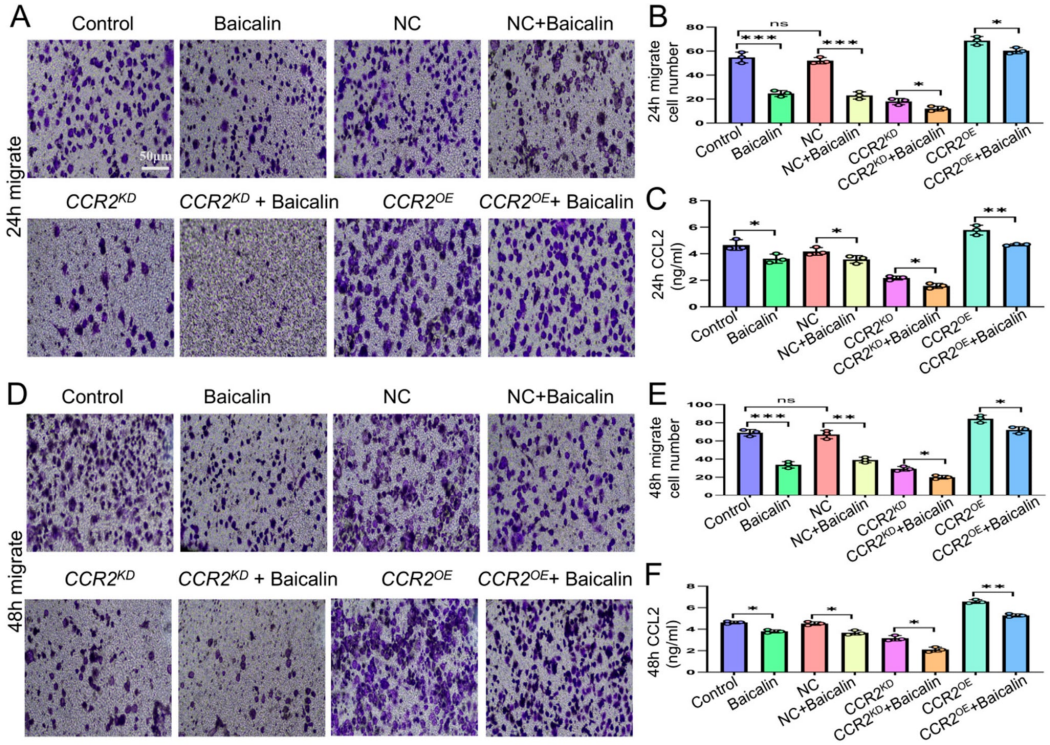


Figure 5. Baicalin-pretreated RA-FLSs suppress macrophage migration via CCL2/CCR2 axis. (**A**) Representative images of cell migration over 24 h for each group: Control (wild-type J774A.1 + untreated RA-FLSs); Baicalin (wild-type J774A.1 + baicalin-pretreated RA-FLSs); NC (negative control lentivirus-transfected J774A.1 + untreated RA-FLSs); NC + Baicalin (negative control lentivirus-transfected J774A.1 + baicalin-pretreated RA-FLSs); $CCR2^{KD}$ ($CCR2^{KD}$J774A.1 + untreated RA-FLSs); $CCR2^{KD}$ + Baicalin ($CCR2^{KD}$J774A.1 + baicalin-pretreated RA-FLSs); $CCR2^{OE}$ ($CCR2^{OE}$J774A.1 + untreated RA-FLS); $CCR2^{OE}$ + Baicalin ($CCR2^{OE}$ J774A.1 + baicalin-pretreated RA-FLSs). (**B**) Quantification of migrated macrophages after 24 h of co-culture. (**C**) CCL2 concentrations in the co-culture supernatant at 24 h. (**D**) Representative images of cell migration at 48 h for each group. (**E**) Quantification of migrated macrophages after 48 h of co-culture. (**F**) CCL2 concentrations in the co-culture supernatant at 48 h. * $p < 0.05$, ** $p < 0.01$, *** $p < 0.001$; ns, not significant.

3.5. Baicalin-Pretreated M1 Macrophages Suppress Secretion of Inflammation-Related Factors from FLS-RAs via the CCL2–CCR2–MAPK/NF-κB Signaling Axis

J774A.1 cells stimulated with 10 pg/mL LPS and 20 ng/mL IFN-γ for 48 h were successfully polarized toward the M1 macrophage phenotype (Figure 6A). ELISA measurements of the IL-6, IL-10, and CCL2 concentrations in the culture supernatants revealed that, compared with the 0 μg/mL baicalin group (Control group), the levels of IL-6 and CCL2 were signifi-

cantly downregulated, whereas IL-10 was markedly upregulated in both the 25 μg/mL and 50 μg/mL baicalin groups (Figure 6B). Western blotting analysis of RA-FLSs further verified that both baicalin concentrations downregulated the protein expressions of CCR2, NF-κB, p-P38/P38, p-JNK/JNK and p-ERK/ERK relative to blank controls (Figure 6C). These results demonstrate that baicalin-pretreated M1 macrophages suppress proinflammatory cytokine secretion from RA-FLSs via the CCL2–CCR2–MAPK/NF-κB signaling axis.

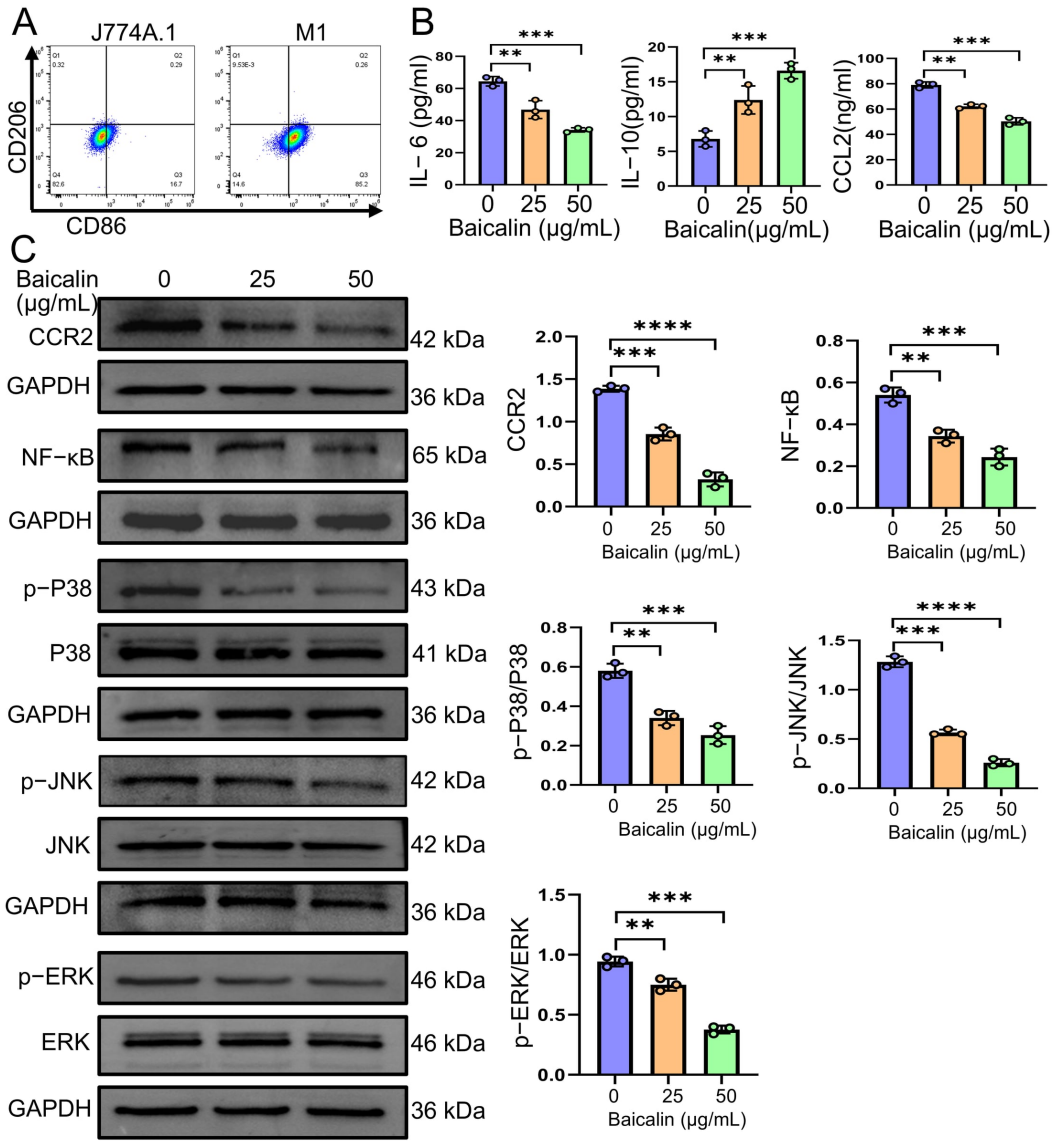


Figure 6. Baicalin-pretreated M1 macrophages suppress inflammation-related factor secretion from FLS-RAs via the CCL2–CCR2–MAPK/NF-κB signaling axis. (**A**) M1 macrophages were successfully induced. (**B**) Concentrations of IL-6, IL-10 and CCL2 in co-culture supernatant. (**C**) Protein expression levels of key components in the CCL2/CCR2/MAPK/NF-κB axis in FLS-RAs: CCR2, NF-κB, p-P38/P38, p-JNK/JNK and p-ERK/ERK. ** $p < 0.01$, *** $p < 0.001$, **** $p < 0.0001$ vs. control group.

3.6. Baicalin-Pretreated RA-FLSs Suppress Secretion of Inflammation-Related Factors from M1 Macrophages via the CCL2–CCR2–MAPK/NF-κB Signaling Axis

RA-FLSs maintained good cellular status following continuous 72 h treatment with baicalin at 25 μg/mL or 50 μg/mL (Figure 7A) Following 48 h of co-culture, the ELISA quantification of IL-6, IL-10, and CCL2 in co-culture supernatants showed that, compared with the control group (0 μg/mL baicalin group), the concentrations of IL-6 and CCL2 were significantly decreased, while IL-10 was markedly elevated in both the 25 μg/mL and 50 μg/mL

baicalin groups (Figure 7B). Western blotting analysis of M1 macrophages further confirmed that baicalin at both concentrations reduced the protein levels of CCR2, NF-κB, p-P38/P38, p-JNK/JNK and p-ERK/ERK relative to the control group (Figure 7C). These findings indicate that baicalin-pretreated RA-FLSs inhibit the secretion of inflammation-associated factors by M1 macrophages through the CCL2–CCR2–MAPK/NF-κB signaling axis.

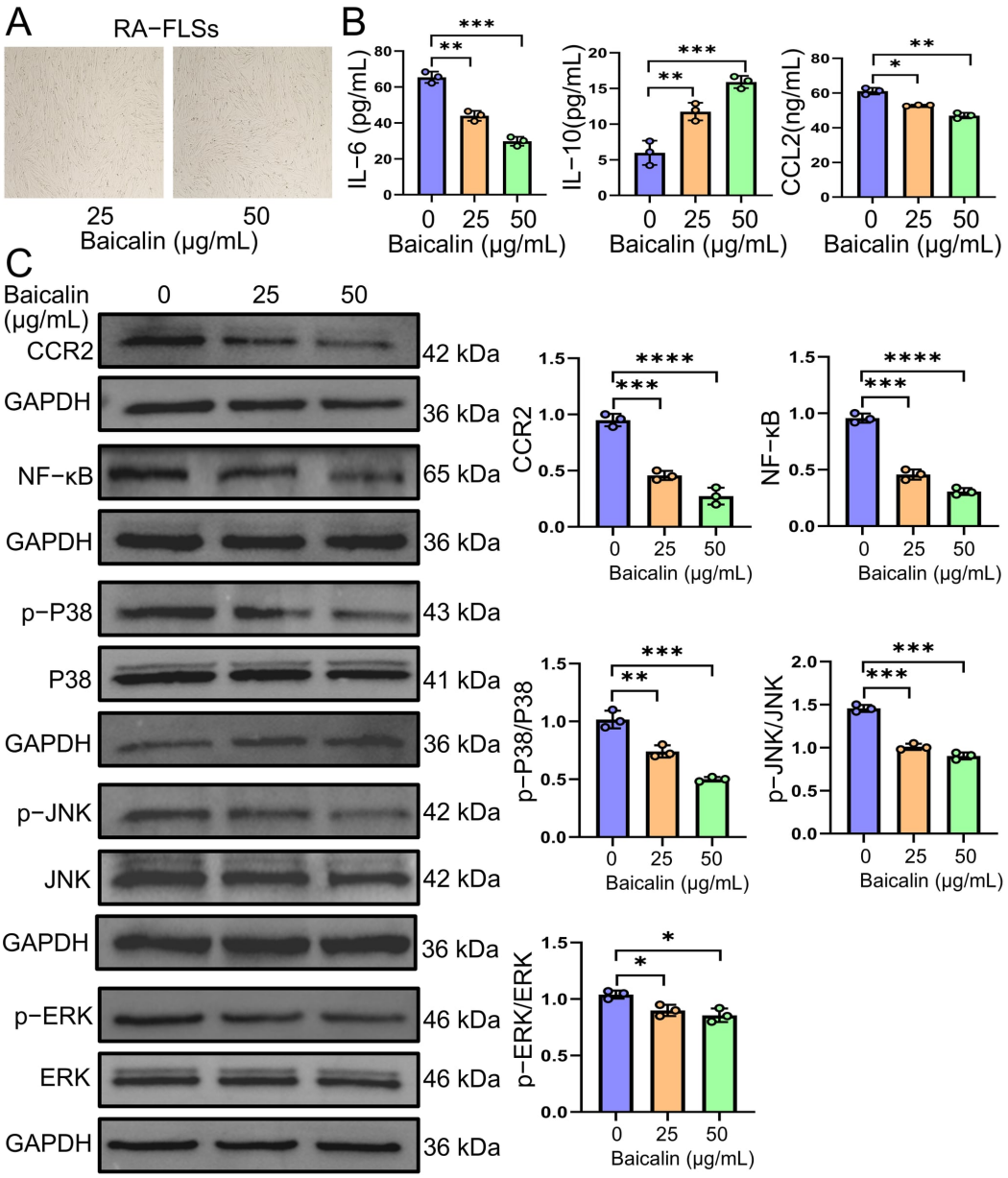


Figure 7. Baicalin-pretreated RA-FLSs suppress inflammation-related factor secretion from M1 macrophages via the CCL2–CCR2–MAPK/NF-κB signaling axis. (**A**) Status of RA-FLSs following continuous 72 h treatment with 25 μg/mL or 50 μg/mL baicalin. (**B**) Concentrations of IL-6, IL-10 and CCL2 in co-culture supernatant. (**C**) Protein expression levels of key components in the CCL2–CCR2–MAPK/NF-κB axis in M1 macrophages. CCR2, NF-κB, p-P38/P38, p-JNK/JNK and p-ERK/ERK. * $p < 0.05$, ** $p < 0.01$, *** $p < 0.001$, **** $p < 0.0001$ vs. control group.

4. Discussion

Rheumatoid arthritis (RA) is a chronic progressive inflammatory disorder characterized by symmetric polyarthritis, which can cause joint and periarticular structural injury as well as systemic inflammatory sequelae [34,35]. Mounting evidence indicates that aberrant

activation of RA-FLSs and synovial macrophages, together with their synergistic proinflammatory crosstalk, drives persistent synovial inflammation, excessive cytokine production, and irreversible joint destruction [36,37].

The CCL2–CCR2 cascade acts as a key upstream controller of macrophage migration and inflammatory activation, with MAPK and NF-κB serving as central downstream signaling nodes [38,39]. Accordingly, the integrated CCL2–CCR2–MAPK/NF-κB axis critically governs RA progression [19]. This study therefore explored whether baicalin inhibits crosstalk between RA-FLSs and synovial macrophages via this signaling cascade. In vivo assays showed that baicalin's anti-arthritic effect is closely linked to the suppression of CCL2–CCR2–MAPK/NF-κB overactivation and promotion of anti-inflammatory M2 macrophage polarization.

To clarify whether baicalin reduces CCL2 secretion from RA-FLSs and thereby restrains macrophage migration through CCL2–CCR2 signaling, we established macrophage lines with stable CCR2 knockdown ($CCR2^{KD}$) and overexpression ($CCR2^{OE}$). Baicalin-pretreated RA-FLSs were co-cultured with macrophages for 24 h and 48 h. Transwell results demonstrated suppressed migration of both $CCR2^{KD}$ and $CCR2^{OE}$ macrophages at both time points, indicating that baicalin inhibits RA-FLS CCL2 secretion and blocks macrophage recruitment via the CCL2–CCR2 axis.

We next examined whether baicalin interrupted RA-FLS–macrophage crosstalk through the CCL2–CCR2–MAPK/NF-κB network using M1-polarized macrophages in two co-culture settings.

First, M1 macrophages were treated with baicalin (25 and 50 μg/mL) for 72 h before co-culture with RA-FLSs. The supernatant exhibited lower CCL2 and IL-6, and higher IL-10. In RA-FLSs, CCR2 expression and the phosphorylation ratios of p-p38/p38, p-ERK/ERK, and p-JNK/JNK, as well as NF-κB-p65, were downregulated. These data show that baicalin-treated macrophages reduce CCL2 and proinflammatory cytokine release from RA-FLSs by targeting the CCL2–CCR2–MAPK/NF-κB axis.

Second, RA-FLSs were pretreated with baicalin (25 and 50 μg/mL) for 72 h and then co-cultured with M1 macrophages for 48 h. Supernatant CCL2 and IL-6 decreased while IL-10 increased. In M1 macrophages, CCR2; NF-κB-p65; and the phosphorylation levels of p38, ERK, and JNK were also reduced. This confirms that baicalin-exposed RA-FLSs suppress CCL2 and proinflammatory cytokine production by macrophages via the same cascade.

Herein, we describe a novel mechanism by which baicalin mitigates RA: the disruption of CCL2–CCR2–MAPK/NF-κB-mediated reciprocal communication between RA-FLSs and synovial macrophages. Most prior baicalin studies focused on its isolated effects on single cell types or individual pathways [40]. By contrast, our findings highlight that baicalin's therapeutic benefit relies on breaking the paracrine inflammatory loop between RA-FLSs and macrophages, rather than merely inhibiting single inflammatory mediators.

Mechanistically, sustained synovial inflammation in RA depends on reciprocal cell–cell crosstalk [41]. Activated RA-FLSs are a major source of synovial CCL2 [42]. CCL2 binds macrophage CCR2 to trigger MAPK/NF-κB activation, M1 polarization, and proinflammatory cytokine release; these mediators further activate RA-FLSs and accelerate synovial hyperplasia and inflammatory infiltration. In CIA rats, baicalin alleviated joint inflammation and bone erosion, suppressed CCL2–CCR2–MAPK/NF-κB signaling, reduced M1 infiltration, and shifted synovial macrophages toward an M2 phenotype. These in vivo observations support the baicalin-mediated regulation of macrophage polarization and CCL2–CCR2 signaling in arthritic joints. In vitro co-culture experiments further dissected this cell interaction, confirming that baicalin inhibits RA-FLS CCL2 secretion. This blockade disrupts CCL2–CCR2-dependent RA-FLS–macrophage communication and limits macrophage recruitment and cytokine release. Collectively, in vivo data reveal pathway and

phenotypic changes in intact joints, while in vitro assays identify RA-FLS-derived CCL2 as a key mediator of macrophage activation. Together, our results support a unified cascade: baicalin inhibits CCL2 release from RA-FLSs, interrupts RA-FLS–macrophage crosstalk via CCL2–CCR2, remodels macrophage polarization, and ultimately ameliorates CIA.

Several limitations of this study should be noted. First, we adopted a cross-species co-culture system using human RA-FLSs and murine J774A.1 macrophages. Interspecies differences in ligand–receptor affinity, cytokine interactions, and downstream signaling may alter cell communication fidelity, so this system cannot fully recapitulate the native inflammatory microenvironment of human RA synovium. Second, spleen-derived macrophages instead of primary synovial macrophages were used for phenotypic detection. Although spleen macrophages reflect systemic immune changes in CIA rats, they do not recapitulate the unique features of synovium-resident macrophages. Third, while the CIA rat model reproduces core RA pathologies including synovial hyperplasia, macrophage infiltration, bone erosion, and CCL2–CCR2 activation, the findings cannot be directly extrapolated to humans. CIA is induced by exogenous type II collagen in inbred rats, whereas human RA is heterogeneous and driven by genetic susceptibility and environmental triggers. Substantial interspecies differences also exist in disease stage, intervention window, immune landscape, and baicalin metabolism. Our results are therefore preclinical mechanistic evidence and require validation with human synovial tissues and clinical studies. Finally, baicalin shows promising anti-arthritic potential via CCL2–CCR2 inhibition, yet safety considerations remain: no obvious toxicity was observed at the tested dose in CIA rats, but its low oral bioavailability, the gap between intraperitoneal and clinical oral administration, and potential interference with physiological CCL2–CCR2 function cannot be ignored. Further pharmacokinetic and toxicological studies are required to evaluate its benefit–risk profile before clinical translation.

In summary, baicalin suppresses aberrant reciprocal crosstalk between RA-FLSs and synovial macrophages by targeting the CCL2–CCR2–MAPK/NF-κB axis. This effect limits excessive macrophage recruitment to the synovium and breaks the synergistic inflammatory loop between RA-FLSs and macrophages, which likely represents the primary mechanism by which baicalin alleviates RA synovitis and joint injury.

Future work will use primary human synovial cells and synovial organoids to reconstruct the three-dimensional human synovial microenvironment [43,44]. This advanced model better recapitulates cell–cell and extracellular matrix crosstalk and overcomes the limitations of conventional cell line co-culture. In addition, subsequent studies will explore crosstalk among multiple inflammatory pathways, pinpoint baicalin's core regulatory nodes within complex molecular networks, and fully elucidate its anti-RA mechanisms.

5. Conclusions

In the present study, experiments using CIA rat models demonstrated that the anti-arthritic effects of baicalin were closely associated with the inhibition of the CCL2–CCR2–MAPK/NF-κB signaling pathway and promotion of macrophage polarization from the M1 toward the M2 phenotype. Subsequent cellular experiments further confirmed that baicalin could disrupt the crosstalk between RA-FLSs and synovial macrophages via the CCL2–CCR2–MAPK/NF-κB signaling network, thereby reducing the excessive release of inflammatory cytokines, which may represent the principal mechanism underlying baicalin-mediated amelioration of RA-associated synovitis and joint damage.

Author Contributions: J.W.: Writing—original draft, Software. M.H.: Formal analysis, Data curation. H.H.: Investigation, Formal analysis. W.Z. (Wenxuan Zhang): Methodology, Formal analysis. Y.Y.: Software, Investigation. W.Z. (Wei Zhang): Investigation, Methodology. W.G.: Conceptualization, Visualization. M.S.: Visualization, Methodology. R.M.: Supervision, Conceptualization. Q.W.: Writing—review & editing, Supervision, Funding acquisition. All authors have read and agreed to the published version of the manuscript.

Funding: The work was supported by the National Natural Science Foundation of China Program (grant No. 82360802).

Institutional Review Board Statement: Male Sprague–Dawley (SD) rats were obtained from the Laboratory Animal Center of Ningxia Medical University (SCXK 2020-0001). All animal procedures were conducted in a specific pathogen-free facility and approved by the Animal Ethics Committee of Ningxia Medical University (2023-N0023, 8 March 2023), following institutional animal welfare guidelines.

Data Availability Statement: The datasets generated and analyzed during the current study are available from the corresponding author on reasonable request.

Acknowledgments: We thank all the members of the Ningxia Key Laboratory of Infection and Immunity for their valuable technical support.

Conflicts of Interest: The authors declare no conflicts of interest.

References

1. Zhao, J.; Guo, S.; Schrodi, S.J.; He, D. Molecular and cellular heterogeneity in rheumatoid arthritis: Mechanisms and clinical implications. *Front. Immunol.* **2021**, *12*, 790122. [CrossRef] [PubMed]
2. Safiri, S.; Kolahi, A.A.; Hoy, D. Global regional and national burden of rheumatoid arthritis 1990-2017: A systematic analysis of the Global Burden of Disease study 2017. *Ann. Rheum. Dis.* **2017**, *78*, 1463–1471.
3. Miguel-Lavariega, D.; Elizararrás-Rivas, J.; Villarreal-Ríos, E. Perfil epidemiológico de la artritis reumatoide [Epidemiological profile of rheumatoid arthritis]. *Rev. Med. Inst. Mex. Seguro Soc.* **2023**, *61*, 574–582. [PubMed]
4. GBD 2021 Rheumatoid Arthritis Collaborators. Global, regional, and national burden of rheumatoid arthritis, 1990-2020, and projections to 2050: A systematic analysis of the Global Burden of Disease Study 2021. *Lancet Rheumatol.* **2023**, *5*, e594–e610. [CrossRef] [PubMed]
5. D'Orazio, A.; Cirillo, A.L.; Greco, G. Pathogenesis of rheumatoid arthritis: One year in review 2024. *Clin. Exp. Rheumatol.* **2023**, *42*, 1707–1713. [CrossRef] [PubMed]
6. McInnes, I.B.; Schett, G. The pathogenesis of rheumatoid arthritis. *N. Engl. J. Med.* **2011**, *365*, 2205–2219. [CrossRef] [PubMed]
7. Zack, S.R.; Alzoubi, O.; Satoeya, N. Another Notch in the Belt of Rheumatoid Arthritis. *Arthritis Rheumatol.* **2024**, *76*, 1475–1487. [CrossRef] [PubMed]
8. Martínez-Ramos, S.; Rafael-Vidal, C.; Marty, J. Semaphorin4B is elevated in rheumatoid arthritis and enhances the inflammatory phenotype of macrophages and fibroblast-like synoviocytes. *Arthritis Res. Ther.* **2025**, *27*, 132. [CrossRef] [PubMed]
9. Wu, M.; Xie, D.; Wang, L. Spatiotemporally targeted nanocapsules combined with mild photothermal therapy regulate the synovial microenvironment in rheumatoid arthritis. *Bioact. Mater.* **2025**, *58*, 33–48. [CrossRef] [PubMed]
10. Kanai, T.; Kondo, N.; Okada, M. The JNK pathway represents a novel target in the treatment of rheumatoid arthritis through the suppression of MMP-3. *J. Orthop. Surg. Res.* **2020**, *15*, 87. [CrossRef] [PubMed]
11. Yin, F.; He, Y.; Li, J.; Gao, Y. Immune cell senescence in autoimmunity: Implications for disease pathogenesis and therapeutic targeting. *Front. Immunol.* **2025**, *16*, 1596686. [CrossRef] [PubMed]
12. Geng, W.; Liu, X.; Tao, B. Nitric Oxide Scavenging and Hydrogen Sulfide Production Synergistically Treat Rheumatoid Arthritis. *Adv. Healthc. Mater.* **2023**, *12*, e2202380. [CrossRef] [PubMed]
13. Zheng, Y.; Wei, K.; Jiang, P. Macrophage polarization in rheumatoid arthritis: Signaling pathways, metabolic reprogramming, and crosstalk with synovial fibroblasts. *Front. Immunol.* **2024**, *15*, 1394108. [CrossRef] [PubMed]
14. Nakamachi, Y.; Uto, K.; Hayashi, S. Exosomes derived from synovial fibroblasts from patients with rheumatoid arthritis promote macrophage migration that can be suppressed by miR-124-3p. *Heliyon* **2023**, *9*, e14986. [CrossRef] [PubMed]
15. Thangadurai, M.; Sethuraman, S.; Subramanian, A. A 2D inflammatory co-culture model for investigating synovial fibroblast and macrophage interactions in rheumatoid arthritis. *Sci. Rep.* **2025**, *15*, 30105. [CrossRef] [PubMed]

16. Fang, F.; Hua, M.; Yu, G. Study of the mechanism of fibroblast-like synoviocytes-derived exosomes inducing macrophages M1 polarization and CD8+ T cells immune regulation ferroptosis and autophagy in rheumatoid arthritis. *Immunol. Lett.* **2024**, *270*, 106936. [CrossRef] [PubMed]
17. Zhang, Z.; Yuan, S.; Ouyang, Y. Targeted delivery of kaempferol via mannose-modified PLGA nanoparticles reprograms macrophages and ameliorates rheumatoid arthritis. *Int. J. Pharm.* **2026**, *9*, 127073. [CrossRef] [PubMed]
18. Hua, P.; Liang, R.; Yang, S. Microneedle-assisted dual delivery of PUMA gene and celastrol for synergistic therapy of rheumatoid arthritis through restoring synovial homeostasis. *Bioact. Mater.* **2024**, *36*, 83–95. [CrossRef] [PubMed]
19. Moadab, F.; Khorramdelazad, H.; Abbasifard, M. Role of CCL2/CCR2 axis in the immunopathogenesis of rheumatoid arthritis: Latest evidence and therapeutic approaches. *Life Sci.* **2021**, *269*, 119034. [CrossRef] [PubMed]
20. Chen, W.; Fang, Y.; Wang, H. Role of chemokine receptor 2 in rheumatoid arthritis: A research update. *Int. Immunopharmacol.* **2023**, *116*, 109755. [CrossRef] [PubMed]
21. Li, R.; Wu, X.; Peng, S. CCR2 antagonist represses fibroblast-like synoviocyte-mediated inflammation in patients with rheumatoid arthritis. *Int. Immunopharmacol.* **2023**, *122*, 110570. [CrossRef] [PubMed]
22. Fan, W.; Xu, Z.; Liang, S. MLL3 Inhibits Apoptosis of Rheumatoid Arthritis Fibroblast-Like Synoviocytes and Promotes Secretion of Inflammatory Factors by Activating CCL2 and the NF-κB Pathway. *Inflammation* **2021**, *44*, 1803–1814. [CrossRef] [PubMed]
23. Zhu, S.; Liu, M.; Bennett, S. The molecular structure and role of CCL2 (MCP-1) and C-C chemokine receptor CCR2 in skeletal biology and diseases. *J. Cell. Physiol.* **2021**, *236*, 7211–7222. [CrossRef] [PubMed]
24. Tang, C.; Tsai, C.C. CCL2 increases MMP-9 expression and cell motility in human chondrosarcoma cells via the Ras/Raf/MEK/ERK/NF-κB signaling pathway. *Biochem. Pharmacol.* **2012**, *83*, 335–344. [CrossRef] [PubMed]
25. Lee, S.H.; Jeong, G.H.; Nam, M.K. Polystyrene microplastics activate NF-κB/MAPK signaling in synovial fibroblasts, promoting inflammation and joint destruction in rheumatoid arthritis. *J. Hazard. Mater.* **2025**, *499*, 140194. [CrossRef] [PubMed]
26. Chang, J.; Liu, S.; Lin, Y. Nesfatin-1 Stimulates CCL2-dependent Monocyte Migration and M1 Macrophage Polarization: Implications for Rheumatoid Arthritis Therapy. *Int. J. Biol. Sci.* **2023**, *19*, 281–293. [CrossRef] [PubMed]
27. Katturajan, R.S.V.; Rasool, M.; Evan Prince, S. Molecular toxicity of methotrexate in rheumatoid arthritis treatment: A novel perspective and therapeutic implications. *Toxicology* **2021**, *461*, 152909. [CrossRef] [PubMed]
28. Retuerto, M.; Trujillo, E.; Valero, C. Efficacy and safety of switching Jak inhibitors in rheumatoid arthritis: An observational study. *Clin. Exp. Rheumatol.* **2021**, *39*, 453–455. [CrossRef] [PubMed]
29. Zhang, S.; Zhong, R.; Zhou, M. Mechanisms of Baicalin Alleviates Intestinal Inflammation: Role of M1 Macrophage Polarization and Lactobacillus amylovorus. *Adv. Sci.* **2025**, *12*, e2415948. [CrossRef] [PubMed]
30. Pan, Y.; Shi, Z.; Wang, Y. Baicalin promotes β-1,3-glucan exposure in Candida albicans and enhances macrophage response. *Front. Cell. Infect. Microbiol.* **2024**, *14*, 1487173. [CrossRef] [PubMed]
31. Sun, Y.; Liu, J.; He, M.; Chen, X. Baicalin improves the inflammatory response of RA-FLS by targeting the circ_0000734/miR-197-5p/IKBKB axis. *Front. Immunol.* **2026**, *17*, 1828868. [CrossRef] [PubMed]
32. Bai, L.; Bai, Y.; Yang, Y. Baicalin alleviates collagen-induced arthritis and suppresses TLR2/MYD88/NF-κB p65 signaling in rats and HFLS-RAs. *Mol. Med. Rep.* **2020**, *22*, 2833–2841. [CrossRef] [PubMed]
33. Yang, Y.; Li, H.; Bai, L. Bioinformatics analysis of ceRNA regulatory network of baicalin in alleviating pathological joint alterations in CIA rats. *Eur. J. Pharmacol.* **2023**, *951*, 175757. [CrossRef] [PubMed]
34. Myasoedova, E. Rheumatoid Arthritis Before and Beyond the Joint: Early Recognition, Targeted Treatment, and Primary Care Co-Management. *Mayo Clin. Proc.* 2026, *in press*.
35. Yue, S.; Fan, J.; Xie, D.; Cao, C.; Wang, Z.; Huang, J.; Qiu, F.; Yang, X.; He, D.; Lu, A.; et al. Unveiling the Therapeutic Potential: Targeting Fibroblast-like Synoviocytes in Rheumatoid Arthritis. *Expert Rev. Mol. Med.* **2025**, *27*, e18. [CrossRef] [PubMed]
36. Ganeshalingam, S.; Wilson, N.J.; Ciciriello, S. Cellular interactions in maintaining an inflammatory microenvironment in rheumatoid arthritis. *Mol. Immunol.* **2025**, *184*, 112–122. [CrossRef] [PubMed]
37. Cai, M.; Li, Z.; Wen, X. C3a-C3aR1-Mediated Interactions Between Fibroblast Like Synoviocytes and Macrophages Promote the Progression of Rheumatoid Arthritis. *Arthritis Rheumatol.* **2025**, *77*, 1697–1712. [CrossRef] [PubMed]
38. Wang, Q.; Liu, F.; Li, Y. Choroid plexus CCL2-CCR2 signaling orchestrates macrophage recruitment and cerebrospinal fluid hypersecretion in hydrocephalus. *Acta Pharm. Sin. B* **2024**, *14*, 4544–4559. [CrossRef] [PubMed]
39. Fan, M.; Liang, Z.; Shen, J. The function of chemokine-driven glial-neuronal interaction in chronic pain. *Front. Neurosci.* **2026**, *20*, 1830053. [CrossRef] [PubMed]
40. Wang, L.; Yao, S.; Wang, J. Integrated Analysis of Proteomics and Metabolomics Uncovered the Anti-Inflammatory Mechanisms of Baicalin in CIA Rat FLS. *Curr. Issues Mol. Biol.* **2026**, *48*, 111. [CrossRef] [PubMed]
41. Tu, J.; Huang, W.; Zhang, W. Two Main Cellular Components in Rheumatoid Arthritis: Communication Between T Cells and Fibroblast-Like Synoviocytes in the Joint Synovium. *Front. Immunol.* **2022**, *13*, 922111. [CrossRef] [PubMed]

42. Corrigall, V.M.; Arastu, M.; Khan, S. Functional IL-2 receptor beta (CD122) and gamma (CD132) chains are expressed by fibroblast-like synoviocytes: Activation by IL-2 stimulates monocyte chemoattractant protein-1 production. *J. Immunol.* **2001**, *166*, 4141–4147. [CrossRef] [PubMed]
43. Wang, X.; He, J.; Zhang, Q. Constructing a 3D co-culture in vitro synovial tissue model for rheumatoid arthritis research. *Mater. Today Bio* **2025**, *31*, 101492. [CrossRef] [PubMed]
44. Zhou, H.; Zhang, Z.; Mu, Y. 3D Bioprinted Human Synovium-Cartilage Models Mimic Rheumatoid Arthritis Microenvironment and Recapitulate In Vivo Therapeutic Responses. *Adv. Mater.* **2026**, *38*, e13952. [CrossRef] [PubMed]

Disclaimer/Publisher's Note: The statements, opinions and data contained in all publications are solely those of the individual author(s) and contributor(s) and not of MDPI and/or the editor(s). MDPI and/or the editor(s) disclaim responsibility for any injury to people or property resulting from any ideas, methods, instructions or products referred to in the content.